Abbreviations

%N	percentage nitrogen by mass
a.u.	atomic units
B3LYP	Becke, 3-parameter, Lee-Yang-Parr hybrid functional
BCP	bonding critical point
CH$_3$CH$_3$	NC repeat unit with two methoxy capping groups
CH$_3$OH	NC repeat unit with methoxy capping group on ring 1, hydroxy group on ring 2
CCP	cage critical point
CP	critical point
DFT	density functional theory
DOS	degree of substitution
EM	energetic materials
ESP	electrostatic potential
G09	Gaussian 09 revision D.01
GM	genetically modified
GView	Gauss View 5.0.8
HF	Hartree Fock theory
IR	infra-red spectroscopy

MEP	minimum energy path
MM	molecular mechanics
MMFF94	Merck molecular force field 94
MW	molecular weight
NC	nitrocellulose
NCP	nuclear critical point
NG	nitroglycerine
NMR	nuclear magnetic resonance spectroscopy
OHCH$_3$	NC repeat unit with hydroxy capping group on ring 1, methoxy group on ring 2
PCM	polarisable continuum model
PES	potential energy surface
PETN	pentaerythritol tetranitrate
QM	quantum mechanics
QTAIM	quantum theory of atoms in molecules
RCP	ring critical point
SB59	1,4-bis(ethylamino)-9,10-anthraquinone dye
SEM	scanning electron microscopy
S$_N$2	bi-molecular nucleophilic substitution reaction
TS	transition state
UFF	universal force field
UV	ultraviolet
UV-Vis	ultraviolet–visible spectroscopy
ωB97X-D	ωB97X-D long-range corrected hybrid functional

Chapter 2

Nitration and Denitration Sequence of Nitrocellulose

[Added as preamble for Chapter 4 below]

2.1   Introduction

Moniruzzaman *et al.* used the UV absorption of an anthraquinone dye to determine the activation energies for the removal of the nitrate at C2, C3, C6 sites on nitrocellulose (NC) (figure 2.1)[1]. The reaction of the released NO_x with the 1,4-bis(ethylamino)-9,10-anthraquinone dye (SB59) mimics the action of stabilisers within NC formulations. The dye consumes any nitrates released in the system, eliminating the possibility of further reactions generating acidic species. The presence of acids has been linked to autocatalytic rates of degradation in later stages of NC decomposition[2, 3, 4, 5]. Un-aged NC thin films and films aged at 40°C, 50°C, 60°C and 70°C for timescales of up to 2000hrs for 40°C, were compared. The NC starting material was 12.15%N by mass, indicating that individual glucopyranose rings were of non-uniform, mixed nitration level. Mean degree of substitution (DOS) was 2.307.

The study found that the nitrate at the C3 position would be most reactive, possessing the lowest activation barrier to removal *via* thermolysis. This was followed by C2 and C6. The findings contrast with the work of Shukla *et al.* which determined that denitration via alkyaline hydrolysis followed the order of C3→C6→C2 [6, 7]. However, Shukla's study considered only the fully nitrated system. There is evidence that nitration and denitration is influenced by the presence of nitrate groups at adjacent positions. Matveev *et al.* demonstrated that for polynitro esters the rate of liquid-phase decomposition did not increase linearly with number of nitrate reaction centres.[8]. It was suggested that the trend
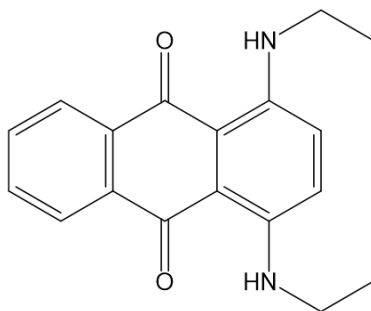
Figure 2.1: 1,4-bis(ethylamino)-9,10-anthraquinone dye (SB59) used to probe the release of nitrates from NC using UV-Vis spectroscopy and ^{1}H NMR[1]. Following reaction with NO_x the UV absorption peak of the dye shifts, indicating the extent of denitration and the presence of secondary reaction products.

in reactivity could be explained by the inductive effect of nitrate groups. The inductive effect arises when a difference in the electronegativity between atoms connected by a *s*-bond causes a polarisation, or permanenet dipole, in the bond. Electron donating groupsincrease the *d*- partial charge on neighbouring atoms through the release of electrons, and electron withdrawing groups pull electron density away from neighbouring atoms generating a *d*+ charge. This suggests that the denitration order could vary with the mechanism of denitration, DOS of the NC, and distribution of the nitrate groups along the polymer.

Chapter 4

Post-Denitration Reactions

4.1 Introduction

[Excerpt from Section 2.1 added above, so the below paragraph makes sense.]

Following the initial denitration step, products are evolved as gases or remain in the NC matrix. Reactive nitrogen dioxide radicals generated from homolysis of the O-N bond not evolved as NO_2 gas, are likely to migrate within the bulk and attack other sites in the polymer and free species. Nitrous acid released from intramolecular reactions within the polymer contribute to the acidity of the overall system, lowering the pH and further stimulating hydrolysis processes.

The neutral and alkaline hydrolysis reactions follow a pseudo-first order process. The degradation of cellulose also follows a pseudo-first order rate[9]. As described in section 2.1, Moniruzzaman *et al.* analysed the reaction of nitrates with anthraquinone dye SB59 to probe the reactivity at each of the C2, C3 and C6 sites on NC, using ultraviolet–visible spectroscopy (UV-Vis) and H NMR spectra (figure 4.1). In the study, the presence of secondary reaction products following the liberation of the nitrate group was observed in the UV-Vis absorption spectra. Samples with longer ageing time presented spectra dominated by consecutive products. Though figure 4.1 illustrates the reaction of the dye with NO groups, the study makes no indication of the source of NO_x, except that they are products of thermolysis of NC.

In this section, secondary and extended reaction schemes for the low temperature ageing of NC are explored. Mechanisms proposed by Camera *et al.* and Aellig *et al.* are probed to determine the reactions responsible for the experimentally observed degradation products.
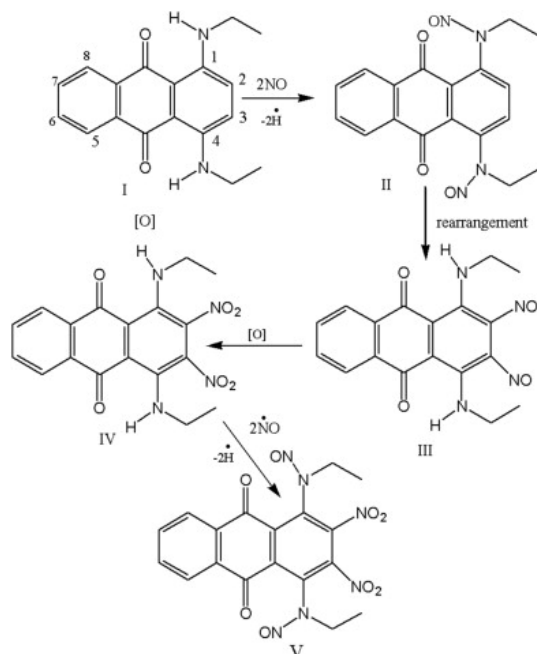
Figure 4.1: Proposed reaction pathway for anthraquinone dye (SB59) with NOx released as a result of denitration, from the work of Moniruzzaman *et al.*[1].

4.2   Methodology

The species reactions proposed by Camera and Aellig *et al.* were geometry optimised using ωB97X-D long-range corrected hybrid functional (ωB97X-D), and Becke, 3-parameter, Lee-Yang-Parr hybrid functional (B3LYP) functionals. The reactions were initally modelled using ethyl nitrate as a test system before expansion to the full C2 monomer.

4.2.1   Computational details

All geometry optimisations were performed in Gaussian 09 revision D.01 (G09), using the ωB97X-D and B3LYP functionals. Optimisations were repeated with polarisable continuum model (PCM) to introduce solvent effects.

4.3   Results and Discussion

4.3.1   Thermodynamics of Ethyl Nitrate reactions
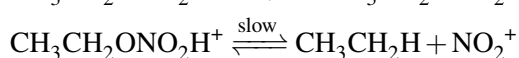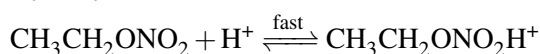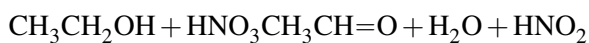
Camera' equations

Hydrolysis

$$CH_3CH_2ONO_2 + H^+ \underset{}{\overset{fast}{\rightleftharpoons}} CH_3CH_2ONO_2H^+$$

$$CH_3CH_2ONO_2H^+ \underset{}{\overset{slow}{\rightleftharpoons}} CH_3CH_2H + NO_2{}^+$$

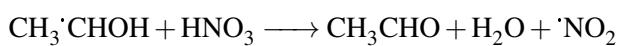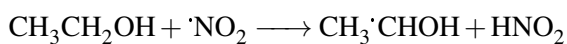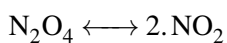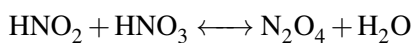$$NO_2{}^+ + 2\,H_2O \underset{}{\overset{fast}{\rightleftharpoons}} HNO_3 + H_3O^+$$
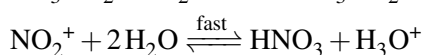
Table 4.1: Reaction energies of reactions following denitration. Calculations carried out at 6-31+G(2df,p) level and solvent PCM was implemented.

Reaction		ΔG_r			
	ΔH_r	ωB97X-D	PCM	B3LYP	PCM
1 $CH_3CH_2ONO_2 + H_2O \longrightarrow CH_3CH_2OH + HNO_3$		0.0072	0.0083	0.0064	0.0077
2 $CH_3CH_2ONO_2 + H_3O^+ \longleftrightarrow CH_3CH_2ONO_2H^+ + H_2O$		-0.0195	0.0140	-0.0219	0.0101

Initiation

$$CH_3CH_2OH + HNO_3 CH_3CH=O + H_2O + HNO_2$$

Propagation

$$HNO_2 + HNO_3 \longleftrightarrow N_2O_4 + H_2O$$

$$N_2O_4 \longleftrightarrow 2\,.NO_2$$

$$CH_3CH_2OH + \dot{}NO_2 \longrightarrow CH_3\dot{}CHOH + HNO_2$$

$$CH_3\dot{}CHOH + HNO_3 \longrightarrow CH_3CHO + H_2O + \dot{}NO_2$$

Aellig's equations

Initiation

$$4\,HNO_3 \rightleftharpoons 4\,NO_2 + 2\,H_2O + O_2$$

$$2\,NO_2 + H_2O \rightleftharpoons N_2O_4 + H_2O$$

$$N_2O_4 + H_2O \longrightarrow HNO_3 + HNO_2$$

Propagation

$$CH_3CH_2OH + HNO_2 \longleftrightarrow CH_3CH_2ONO + H_2O$$

$$CH_3CH_2ONO \longrightarrow CH_3CH=O + HNO$$

$$\dot{}NO_2 + HNO \longrightarrow HNO_2 + \dot{}NO$$

$$2\,\dot{}NO + O_2 \longrightarrow 2\,\dot{}NO_2$$

Termination

$$HNO + HNO \longrightarrow HON=NOH$$

$$HON=NOH \longrightarrow N_2O + H_2O$$
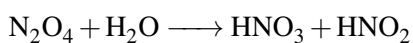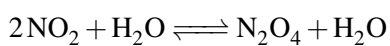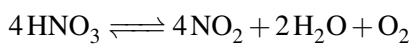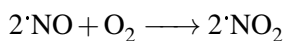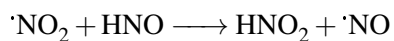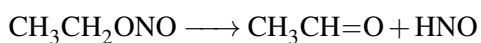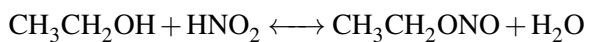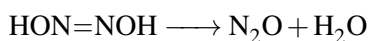
4.3.1.1   Radical mechanistic route

4.3.1.2   Ionic mechanistic route

4.3.2   Reactions of Nitrocellulose Monomer

4.4   Summary

Bibliography

[1] Mohammed Moniruzzaman, John M. Bellerby, and Manfred A. Bohn. Activation energies for the decomposition of nitrate ester groups at the anhydroglucopyranose ring positions C2, C3 and C6 of nitrocellulose using the nitration of a dye as probe. *Polymer Degradation and Stability*, 102:49–58, apr 2014.

[2] M. Edge, N.S. Allen, M. Hayes, P.N.K. Riley, C.V. Horie, and J. Luc-Gardette. Mechanisms of deterioration in cellulose nitrate base archival cinematograph film. *European Polymer Journal*, 26(6):623–630, jan 1990.

[3] Mª Ángeles Fernández de la Ossa, María López-López, Mercedes Torre, and Carmen García-Ruiz. Analytical techniques in the study of highly-nitrated nitrocellulose. *TrAC Trends in Analytical Chemistry*, 30(11):1740–1755, dec 2011.

[4] John W. Baker and D. M. Easty. Hydrolytic decomposition of esters of nitric acid. Part I. General experimental techniques. Alkaline hydrolysis and neutral solvolysis of methyl, ethyl, isopropyl, and tert.-butyl nitrates in aqueous alcohol. *Journal of the Chemical Society (Resumed)*, 1952(0):1193–1207, 1952.

[5] N. Binke, L. Rong, Y. Zhengquan, W. Yuan, Y. Pu, Hu Rongzu, and Y. Qingsen. Studies on the Kinetics of the First Order Autocatalytic Decomposition Reaction of Highly Nitrated Nitrocellulose. *Journal of Thermal Analysis and Calorimetry*, 58(2):403–411, 1999.

[6] Manoj K. Shukla and Frances Hill. Theoretical investigation of reaction mechanisms of alkaline hydrolysis of 2,3,6-trinitro-β-d-glucopyranose as a monomer of nitrocellulose. *Structural Chemistry*, 23(6):1905–1920, apr 2012.

[7] Manoj K Shukla and Frances Hill. Computational elucidation of mechanisms of alkaline hydrolysis of nitrocellulose: dimer and trimer models with comparison to the corresponding monomer. *The journal of physical chemistry. A*, 116(29):7746–55, 2012.

[8] V. G. Matveev and G. M. Nazin. Stepwise Degradation of Polyfunctional Compounds. *Kinetics and Catalysis*, 44(6):735–739, nov 2003.

[9] Paolo Calvini, Andrea Gorassini, and Antonio Luigi Merlani. On the kinetics of cellulose degradation: looking beyond the pseudo zero order rate equation. *Cellulose*, 15(2):193–203, apr 2008.